A theoretical resonant-tunnelling approach to electric-field effects in quasiperiodic Fibonacci GaAs-(Ga,Al)As semiconductor superlattices



1998 J. Phys.: Condens. Matter 10 3557

(http://iopscience.iop.org/0953-8984/10/16/009)

J. Phys.: Condens. Matter **10** (1998) 3557–3567. Printed in the UK PII: S0953-8984(98)89642-2

# A theoretical resonant-tunnelling approach to electric-field effects in quasiperiodic Fibonacci GaAs–(Ga,Al)As semiconductor superlattices

E Reyes-Gómez†, C A Perdomo-Leiva†, L E Oliveira‡ and M de Dios-Leyva§

† Departamento de Física, ISPJAE, Calle 127 s/n, Marianao, 19390, Havana, Cuba
‡ Instituto de Física, Unicamp, CP 6165, Campinas, São Paulo, 13083-970, Brazil
§ Department of Theoretical Physics, University of Havana, San Lazaro y L, Vedado, 10400, Havana, Cuba

Received 1 December 1997

**Abstract.** A theoretical resonant-tunnelling approach is used in a detailed study of the electronic and transmission properties of quasiperiodic Fibonacci GaAs–(Ga,Al)As semiconductor superlattices, under applied electric fields. The theoretical scheme is based upon an exact solution of the corresponding Schroedinger equations in different wells and barriers, through the use of Airy functions, and a transfer-matrix technique. The calculated quasibound resonant energies agree quite well with previous theoretical parameter-based results within a tight-binding scheme, in the particular case of isolated Fibonacci building blocks. Theoretical resonant-tunnelling results for $S_4$ and $S_5$ generations of the quasiperiodic Fibonacci superlattice reveal the occurrence of anticrossings of the resonant levels with applied electric fields, together with the conduction- and valence-level wave function localization properties and electric-field-induced migration to specific regions of the semiconductor quasiperiodic heterostructure. Finally, theoretical resonant-tunnelling calculations for the interband transition energies are shown to be in quite good quantitative agreement with previously reported experimental photocurrent measurements.

## 1. Introduction

The physics of semiconductor heterostructures has been of considerable interest in the last two decades both from the fundamental point of view as well as for their potential device applications [1]. In particular, since the experimental realization of quasiperiodic semiconductor superlattices (SLs), such as Fibonacci [2] and Thue–Morse [3] SLs, there has been a growing interest [4–9] in the understanding of their unique physical properties, such as their quasiperiodic electronic and transport properties, as these systems represent intermediate cases between periodic and disordered solids.

Photoluminescence spectroscopy (PLE) techniques were used by Laruelle and Etienne [4], who performed both experimental and theoretical studies of the electronic band structure and wave function localization in GaAs–(Ga,Al)As Fibonacci SLs. Picosecond luminescence and PLE measurements were performed by Yamaguchi *et al* [5], who investigated the electronic structure and perpendicular transport properties of photoexcited carriers in a GaAs–AlAs Fibonacci SL with an enlarged well. The normal-incidence reflectance of GaAs–(Ga,Al)As Fibonacci SLs was studied by Munzar *et al* [6], who

0953-8984/98/163557+11$19.50  

have also performed theoretical calculations, with an envelope-function approach and the renormalization group method, in good agreement with experiment, with their calculations revealing the multifractal properties of the electron energy spectrum and the self-similarity of the wave function of the ground state. Wang and Maan [7] investigated the effects of magnetic fields parallel to the layers in GaAs–(Ga,Al)As Fibonacci SLs, and demonstrated that the cyclotron-orbit centre dispersion of the electron energy levels shows a self-similar or anti-self-similar field-dependent structure for fields related to integer powers of the $\tau$ golden mean. Toet *et al* [8] have measured the magneto-optical absorption spectra of GaAs–(Ga,Al)As Fibonacci SLs with magnetic fields applied parallel to the layers, and suggested that the spectra exhibit self-similarity at magnetic fields scaled by $\tau$. Bruno-Alfonso *et al* [9] have recently calculated the magnetic Landau subbands, wave functions, and intraband and interband absorption coefficients of quasiperiodic GaAs–(Ga,Al)As Fibonacci SLs under in-plane magnetic fields, and showed that, for a given sample and magnetic field, the Landau magnetic subbands exhibit a Fibonacci-like quasiperiodic structure, and that the intraband absorption spectra are either self-similar (for even $n$) or anti-self-similar (for odd $n$) under in-plane magnetic fields scaled by $\tau^{2n}$. They have also shown that the interband absorption spectra are self-similar under fields scaled by $\tau^{2n}$, and that the width of the interband peaks increase linearly with increasing field in agreement with the experimental results by Toet *et al* [8].

The electric-field-induced effects of an external homogeneous electric field $F$ on the electronic structure and optical properties of both periodic [10–20] and quasiperiodic [21–24] semiconductor SLs have also been extensively studied, both experimentally and from the theoretical point of view. For periodic SLs, it has been established [10, 12, 13] that an electric field applied parallel to the SL axis localizes the electron wave functions (Wannier–Stark localization) and that the localization region is a quantity of the order of $\Delta/eF$, where $\Delta$ is the SL miniband energy width, and $-e$ is the electron charge. The electric-field effect results in a discrete electronic spectrum, which consists of equidistant levels (Stark ladder) separated by a distance $eFd$, where $d$ is the SL period. The Wannier–Stark ladder formation has been experimentally realized in GaAs–(Ga,Al)As SLs [11, 16, 18], and its implications on the absorption spectra has been treated by various authors [11, 17]. Other effects such as the interaction between Wannier–Stark states [14], the changes induced by electric fields on the transmission spectrum of an SL [15], and the coherence of the electron wave functions for real SLs have been also considered in the literature [19, 20]. With respect to quasiperiodic SLs, the effects of an external electric field on the electronic and optical properties of a GaAs–(Ga,Al)As $\alpha$-Fibonacci SL were experimentally investigated by Laruelle *et al* [21, 22] using photocurrent spectroscopy. It was shown that the photocurrent spectra are greatly modified by the electric field and that this effect may be explained within a simple tight-binding scheme including only the Fibonacci SL sequence on which the different electronic states are peaked at zero electric field [21, 22]. Theoretical studies of field-induced localization in Fibonacci and Thue–Morse SLs, and of transmission and localization properties of Fibonacci SLs, both in the absence and presence of a electric field, were recently reported by de Brito *et al* [23] and Castro and Domínguez-Adame [24], respectively.

The experimental measurements of Laruelle *et al* [21, 22] on electric-field-induced effects in GaAs–(Ga,Al)As $\alpha$-Fibonacci SLs have motivated the present study, in which we perform a theoretical study of resonant tunnelling in the above semiconductor quasiperiodic heterostructure, and use a transfer-matrix approach to determine the transmissivity of the heterostructure as a function of the incident electron energy. In particular, within this scheme, one calculates the electronic and interband properties by taking into account the

appropriate coupling of the patterns which are present in the actual quasiperiodic $\alpha$-Fibonacci sequence. In that way, one obtains a quite good understanding of several features of the experimental data, as we shall detail below.

The work is organized as follows. In section 2, we detail the theoretical scheme used in the calculations. Section 3 presents the calculated results and discussion. Finally, our conclusions are presented in section 4.

## 2. Theoretical framework

We shall be concerned with Fibonacci GaAs–(Ga,Al)As quasiperiodic semiconductor SLs, obtained by stacking along the growth axis elements (or elementary blocks) A and B, made of semiconductor layers, and obeying the Fibonacci inflation law A $\rightarrow$ AB and B $\rightarrow$ A. The Fibonacci sequence $S_j = S_j(\mathrm{A},\mathrm{B})$ results after $j$ applications of this law, which leads to the recurrent concatenation rule $S_j = S_{j-1}S_{j-2}$ for $j \geqslant 1$, with $S_{-1} = \mathrm{B}$ and $S_0 = \mathrm{A}$. One may then see that the number $F_j$ of elementary blocks in $S_j$ follows the Fibonacci sequence $F_j = F_{j-1} + F_{j-2}$, with $F_{-1} = F_0 = 1$, the ratio $F_j/F_{j-1}$ converges towards the golden mean $\tau = (1+\sqrt{5})/2$ for increasing $j$, and the numbers of elementary blocks A and B in $S_j$ are $F_{j-1}$ and $F_{j-2}$, respectively [25]. In what follows, we will choose the A and B elementary blocks to be made of the same GaAs quantum well (QW) and of a (Ga,Al)As barrier thicker in B than in A ($\alpha$-type [21, 22] Fibonacci SL). In order to compare our theoretical results with the measurements by Laruelle *et al* [21, 22], the quasiperiodic SL elementary blocks are taken as A: 30 Å GaAs, 30 Å $Ga_{0.75}Al_{0.25}As$, and B: 30 Å GaAs, 50 Å $Ga_{0.75}Al_{0.25}As$.

We will use a transfer-matrix technique [26, 27] in the study of the transmissivity of the Fibonacci semiconductor SL of Laruelle *et al* [21, 22]. We consider an $\alpha$-Fibonacci GaAs–(Ga,Al)As semiconductor SL under an externally applied electric field $F$ along the $-z$ growth direction, and take free-field regions at both left and right sides of the heterostructure (see figure 1). In the calculation of the transmissivity, we consider a plane-wave incident

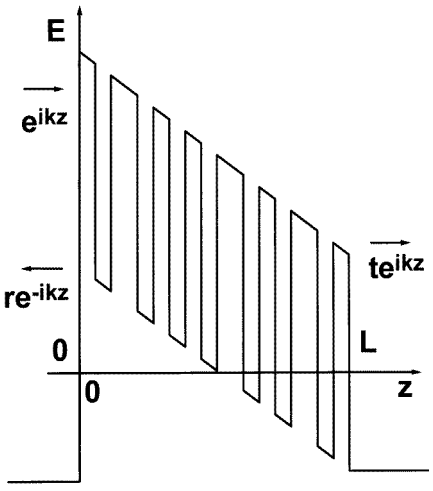


**Figure 1.** Schematic representation of an $\alpha$-Fibonacci GaAs–(Ga,Al)As semiconductor SL potential under an electric field perpendicular to the interfaces and in the $-z$ direction. Also shown are incident, reflected and transmitted plane waves.

from the left, and take the energy origin at the $z_0$ centre of the semiconductor heterostructure, so that the electric-field potential energy is zero at $z = z_0$. In this approach, the resonant energies associated with the peaks in the transmission coefficient for incident electrons and holes may be directly related to the interband-transition energies in the photocurrent experimental results by Laruelle *et al* [21, 22]. The transmissivity for carriers incident from the left of the semiconductor heterostructure may be obtained within a parabolic-band effective-mass scheme [26] in which the $\boldsymbol{k}_\perp \equiv (k_x, k_y) = \mathbf{0}$ envelope $\Psi$ wave function satisfies the following equation,

$$\left[-\frac{\hbar^2}{2}\frac{\mathrm{d}}{\mathrm{d}z}\frac{1}{m(z)}\frac{\mathrm{d}}{\mathrm{d}z} + V(z) - eF(z - z_0)\right]\Psi(z) = E\Psi(z) \tag{2.1}$$

where $V(z)$ is the SL potential, and $m(z)$ is the carrier effective mass, which is taken as $m_b$ in the barriers, and $m_w$ in the wells. The general solution of (2.1) inside any barrier or well in the SL may be written as

$$\Psi_l(z) = C(l)\mathrm{Ai}[u(z, l)] + D(l)\mathrm{Bi}[u(z, l)] \tag{2.2}$$

where

$$u(z, l) = -\frac{z - z_0}{l_F(l)} + \frac{V(l) - E}{\hbar\omega_F(l)} \tag{2.3}$$

$$\omega_F(l) = \left[\frac{e^2F^2}{2\hbar m(l)}\right]^{1/3} \tag{2.4}$$

$$l_F(l) = \left[\frac{\hbar^2}{2eFm(l)}\right]^{1/3} \tag{2.5}$$

and Ai and Bi are the Airy functions. The frequency $\omega_F(l)$ and length $l_F(l)$ are field-dependent characteristic parameters satisfying

$$\hbar\omega_F(l) = eFl_F(l) \tag{2.6}$$

with $l$ used to indicate the specific barrier or well where the above expressions are calculated, with the appropriate values of the potential and effective mass. If one now imposes the continuity of $\Psi_l(z)$ and of $[1/m(z)](\mathrm{d}/\mathrm{d}z)\Psi_l(z)$ at the interfaces between wells and barriers, the $M_n$ transfer matrix, which connects the $C$ and $D$ coefficients in consecutive regions of wells and barriers, may be found. For evaluating the transmissivity, it is also necessary to know the transfer matrices connecting the free-field regions ($z < 0$ and $z > L$, see figure 1) with the regions inside the heterostructure ($0 < z < L$). The full $M^T$ transfer matrix is then given by [26]

$$M^T = -\frac{m_w}{2\mathrm{i}k}\begin{bmatrix} -\mathrm{i}k/m_w & -1 \\ -\mathrm{i}k/m_w & 1 \end{bmatrix} M(0, L) \begin{bmatrix} 1 & 1 \\ \mathrm{i}k/m_w & -\mathrm{i}k/m_w \end{bmatrix} \tag{2.7}$$

where $k$ is the wave vector of the incident carrier, $M(0, L)$ is the transfer matrix between the extremes at $z = 0$ and $z = L$, i.e.,

$$M(0, L) = \prod_{n=N}^{1} M_n. \tag{2.8}$$

It is then straightforward to show that

$$\begin{bmatrix} 1 \\ r \end{bmatrix} = M^T \begin{bmatrix} t \\ 0 \end{bmatrix} \tag{2.9}$$

where 1, $r$ and $t$ are the amplitudes of the incident, reflected and transmitted waves, respectively. Finally, the transmission coefficient is given [26]

$$T = \frac{1}{|M_{11}^T(E)|^2}. \tag{2.10}$$

One should notice that the $M^T$ transfer matrix is a function of the incident carrier energy $E$, and therefore one clearly has the $E$ dependence in the transmission coefficient through (2.10). As is well known [27–29], the transmission coefficient must have sharp peaks for energies near to those of the quasibound states of the heterostructure under applied electric field. In fact, the quasibound-state energies are complex, correspond to the zeros of $M_{11}^T(E)$ in the denominator of (2.10) and may be written as $E = E_0 - \mathrm{i}\Gamma/2$, with $E_0$ and $\Gamma$ corresponding to the energy level and resonance width [29] of the quasibound state.

## 3. Results and discussion

In what follows, the input parameters in the calculations were [4] $m_w/m_0 = 0.067$, and $m_b/m_0 = 0.067 + 0.083x$ for the conduction levels, $m_w/m_0 = 0.34$, and $m_b/m_0 = 0.34 + 0.42x$ for the heavy-hole levels, and $m_w/m_0 = 0.094$, and $m_b/m_0 = 0.094 + 0.056x$ for the light-hole levels. We take the GaAs bulk gap as $E_g = 1.519$ eV, and a 67:33 band-offset ratio with $\Delta E_g(\mathrm{eV}) = 1.247x$, and $x$ being the Al proportion in the barrier.

In order to compare our resonant-tunnelling calculations with the tight-binding results of Laruelle *et al* [22], we have performed calculations for isolated BAB and BAAB patterns, and evaluated the transmission coefficient for incident carriers and various applied electric fields (figures 2(a) and 2(b) for incident electrons), the transmission peak energies for

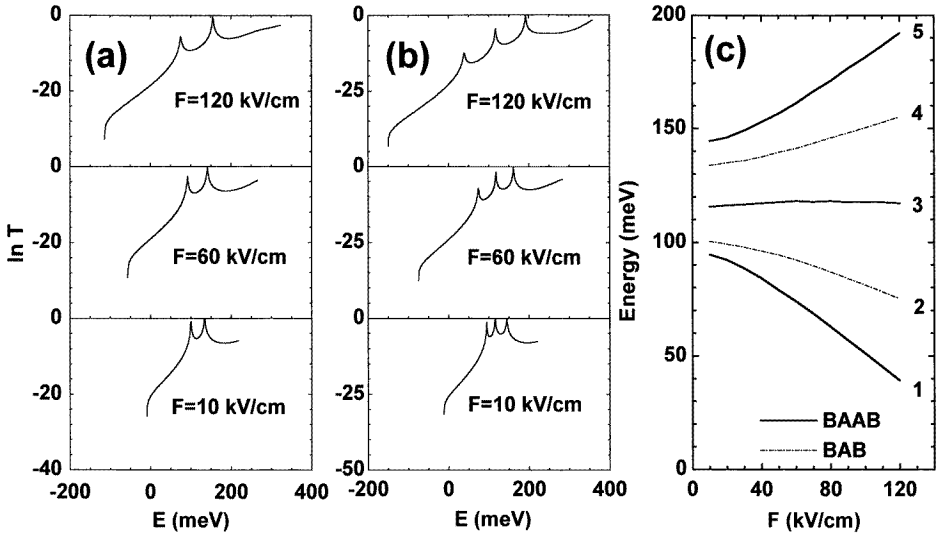


**Figure 2.** Logarithm of the transmission coefficient as a function of incident electron energy for three values of the applied electric field, for the case of either a BAB pattern (a) or a BAAB pattern (b). A and B elements are made of a GaAs QW and a (Ga,Al)As barrier (25% of Al), the barrier being thicker in B than in A (see text). The corresponding transmission peak energies, associated with quasi-resonant states, are shown in (c), for both BAB (dot–dashed curves) and BAAB (full lines) patterns.

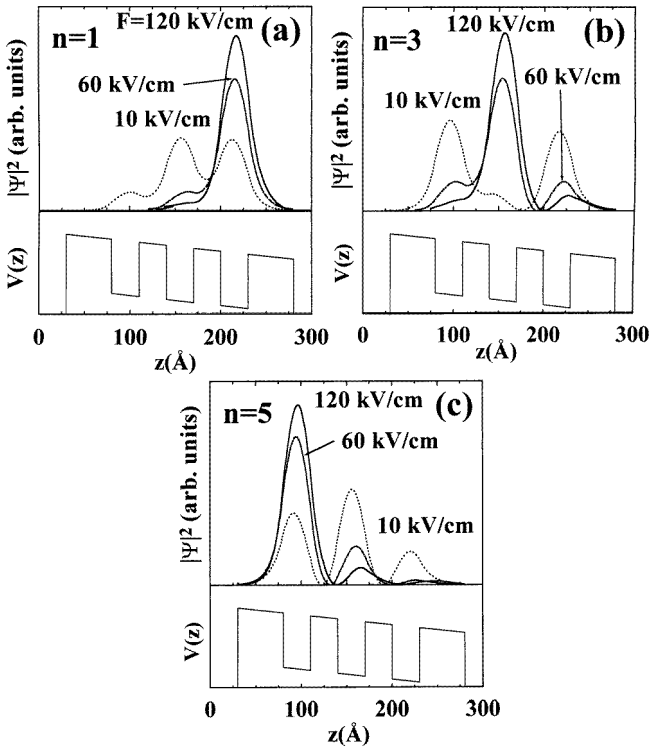


**Figure 3.** Evolution of the square modulus of the BAAB pattern $n = 1$ (a), $n = 3$ (b), and $n = 5$ (c) electron wave functions with applied electric field. A schematic representation of the BAAB-pattern potential is shown in the bottom of each figure.

both patterns (figure 2(c)), the wave function electric-field-dependent localization properties (figure 3), and the interband transition energies as functions of the applied electric field (figure 4). In figure 3, for the BAAB pattern, one clearly sees that the electron wave functions tend to localize in the individual wells of the BAAB pattern with increasing applied electric fields, the same occurring in the case of the BAB pattern. In figure 4, we have used the same labelling for the transitions as Laruelle *et al* [22]: if one denotes by $E_n$ the conduction states, and the heavy-hole and light-hole states by $H_m$ and $L_m$, respectively, and the corresponding transitions are denoted as $E_nH_m$ and $E_nL_m$, then line A is associated with the transition $E_1H_1$, line B with the transition $E_1L_1$, C and D are triplets originating from the transitions $E_2H_2$, $E_1H_3$, $E_3H_1$ and $E_2L_2$, $E_1L_3$, $E_3L_1$, respectively, E and F are each associated with five transitions, $E_2H_4$, $E_1H_5$, $E_3H_3$, $E_4H_2$, $E_5H_1$ and $E_2L_4$, $E_1L_5$, $E_3L_3$, $E_4L_2$, $E_5L_1$, respectively, G and H are related to triplets $E_3H_5$, $E_5H_3$, $E_4H_4$ and $E_3L_5$, $E_5L_3$, $E_4L_4$, respectively, and J and K to the transitions $E_5H_5$ and $E_5L_5$, respectively. Notice that, within the resonant-tunnelling approach, interband transition energies correspond to a summation of the GaAs bulk energy gap with the transmission peak energies (occurying at the quasi-bound energy levels) associated with incident electrons and holes. The good agreement is apparent in figure 4 between the calculations for the interband transition energies within the tight-binding model (we used the same parameters as Laruelle *et al* [22] and reproduced their results) and the results with the resonant-tunnelling approach, indicating that the chosen tight-binding parameters were the appropriate ones.

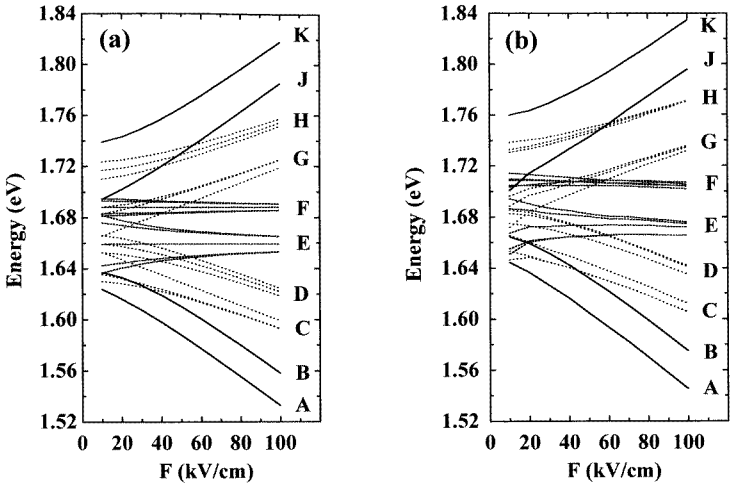


**Figure 4.** Results of the interband transition energies in the case of uncoupled BAB and BAAB patterns as functions of applied electric field: (a) tight-binding model as in Laruelle *et al* [21, 22]; (b) resonant-tunnelling calculation.

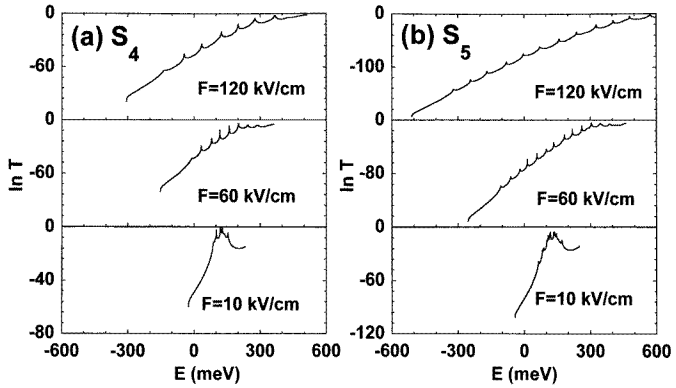


**Figure 5.** Logarithm of the transmission coefficient as a function of incident electron energy for three values of the applied electric field, for the case of either an $S_4$ generation (a) or an $S_5$ generation (b) of an $\alpha$-Fibonacci GaAs–(Ga,Al)As semiconductor SL.

Figure 5 presents the results of our calculations for the electric-field-dependent transmission coefficient as functions of the incident electron energy, in both the cases of the $S_4 =$ ABAABABA and $S_5 =$ ABAABABAABAAB generations of an $\alpha$-Fibonacci GaAs–(Ga,Al)As semiconductor SL. The quasiresonant conduction energy levels (or peaks of the transmission coefficient) are spread apart and strongly coupled for increasing electric fields (cf figure 6(a)), and therefore electric-field effects constitute an adequate tool for probing the multifractal properties of quasiperiodic heterostructure SLs. Figure 6(b) illustrates the change in the spacing between conduction levels $n = 3$ and $n = 4$ with increasing electric field. The electric-field-induced anticrossings between conduction levels $n = 5$ and $n = 6$, and between conduction levels $n = 6$ and $n = 7$, are clearly seen in the evolution of the

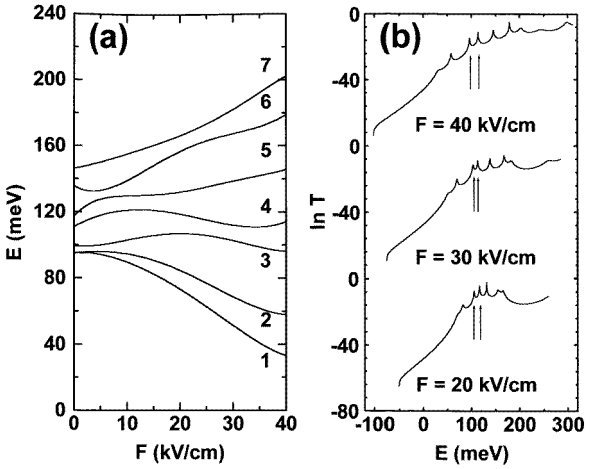


**Figure 6.** (a) Electric-field dependence of the transmission peak energies, associated with quasi-resonant states, and (b) logarithm of the transmission coefficient as a function of incident electron energy for three values of the applied electric field, in the case of an $S_4$ generation of an $\alpha$-Fibonacci GaAs–(Ga,Al)As semiconductor SL. Arrows in (b) indicate evolution with electric field of the $n = 3$ and $n = 4$ conduction peak energies.

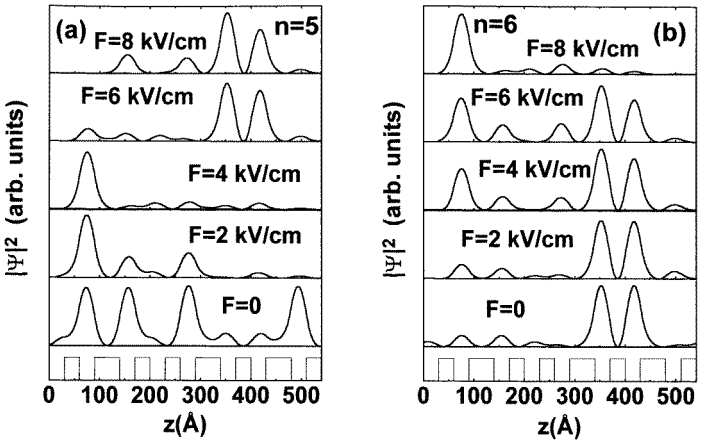


**Figure 7.** Evolution of the square modulus of the $n = 5$ (a), and $n = 6$ (b) electron wave functions (labelled as in figure 6(a)) with applied electric field, in the case of an $S_4$ generation of an $\alpha$-Fibonacci GaAs–(Ga,Al)As semiconductor SL. A schematic representation of the SL potential is shown at the bottom of each figure.

conduction electron wave functions in figures 7 and 8, respectively. Notice that, for high values of the applied electric field (cf figure 8), the electron wave functions tend to localize in the individual wells of the SL, a behaviour already seen in the case of the patterns BAB and BAAB (cf figure 3).

The interband transition energies for the $S_4$ and $S_5$ generations of an $\alpha$-Fibonacci GaAs–(Ga,Al)As semiconductor SL are shown in figure 9, within the resonant-tunnelling approach. Though an exact comparison with the experimental measurements of Laruelle *et al* [21, 22]

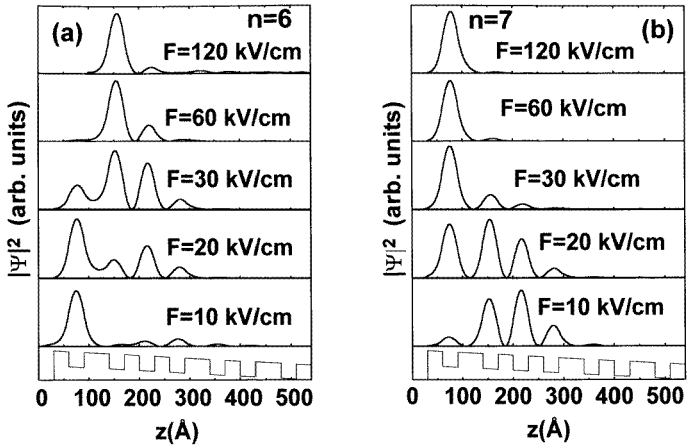


**Figure 8.** Evolution of the square modulus of the $n = 6$ (a), and $n = 7$ (b) electron wave functions (labelled as in figure 6(a)) with applied electric field, in the case of an $S_4$ generation of an $\alpha$-Fibonacci GaAs–(Ga,Al)As semiconductor SL. A schematic representation of the SL potential is shown at the bottom of each figure.

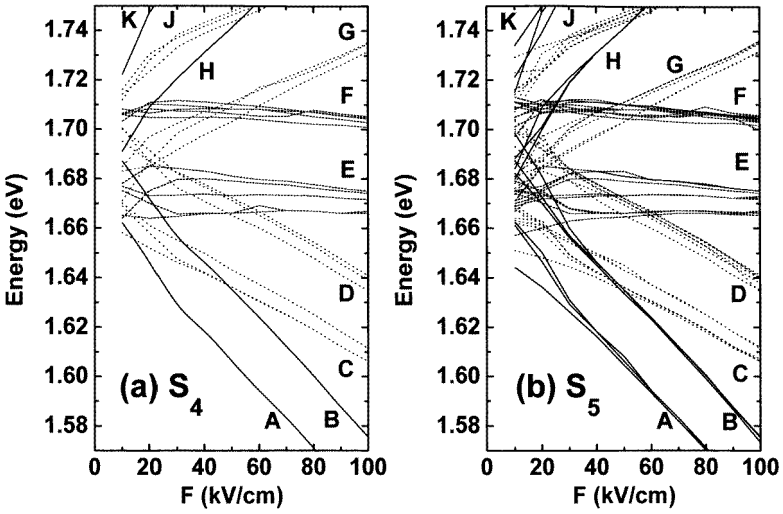


**Figure 9.** Resonant-tunnelling results of the interband transition energies in the case of either an $S_4$ generation (a) or an $S_5$ generation (b) of an $\alpha$-Fibonacci GaAs–(Ga,Al)As semiconductor SL.

is not possible, as their data are for an $S_9$ generation of an $\alpha$-Fibonacci SL, and our calculated results are, for numerical reasons, only for the $S_4$ and $S_5$ generations of the Fibonacci GaAs–(Ga,Al)As SL, one may notice that the essential features of the experiment are present in the resonant-tunnelling calculation. Nevertheless, it is clear from a comparison between the theoretical resonant-tunnelling results for the $S_4$ and $S_5$ generations (cf figure 9) that, for the specific $\alpha$-Fibonacci SL considered, results for intermediate and high values of the applied electric field are only slightly different, and therefore, one should expect that those results

would be a good theoretical approximation for the actual experimental situation [21, 22] of an $S_9$ generation of an $\alpha$-Fibonacci quasiperiodic SL.

Finally, as an illustration, we present in figure 10 the quasibound-state lifetimes, calculated within the resonant-tunnelling approach, for the conduction $n = 3$ resonant state (labelled as in figure 6(a)), in the case of the $S_4$ and $S_5$ generations of an $\alpha$-Fibonacci GaAs–(Ga,Al)As semiconductor SL. One should notice that our results of the order of 0.1–0.4 ps, calculated within the resonant-tunnelling approach, are in qualitative agreement with the theoretical values of 0.12 ps and 0.2 ps reported by Bastard *et al* [14] for a different system, i.e., for semiconductor periodic SLs under electric fields.

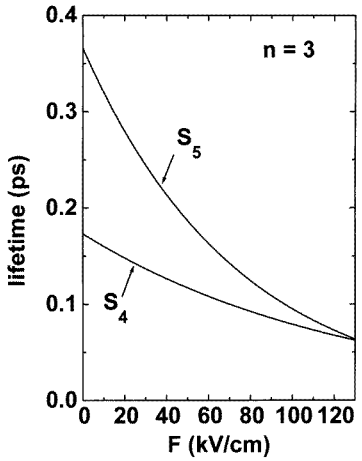


**Figure 10.** Quasibound-state lifetimes for the conduction $n = 3$ resonant state (as in figure 6(a)), in the case of $S_4$ and $S_5$ generations of an $\alpha$-Fibonacci GaAs–(Ga,Al)As semiconductor SL.

## 4. Conclusions

We have presented a quite detailed study of the electronic and transmission properties of $\alpha$-Fibonacci GaAs–(Ga,Al)As semiconductor SLs, under applied electric fields, in which we have used a theoretical resonant-tunnelling approach, based upon an exact solution of the corresponding Schroedinger equation. The calculated quasibound resonant energies agree quite well with previous results based on a simple parameter-based tight-binding scheme, in the case of isolated BAB and BAAB patterns. In addition, we have performed calculations for $S_4$ and $S_5$ generations of the quasiperiodic $\alpha$-Fibonacci SL, in which the anticrossings of the resonant levels with applied electric field may be studied in detail, together with the conduction- and valence-level wave function localization properties and electric-field-induced migration to specific regions of the semiconductor quasiperiodic heterostructure. Moreover, the theoretical resonant-tunnelling results for the interband transition energies are shown to be in quite good quantitative agreement with the experimental photocurrent measurements by Laruelle *et al* [21, 22]. As a final note, one may stress that this resonant-tunnelling approach should be of great value in the quantitative study of how disorder would affect the transmissivity, conductivity and transport properties of systems with applied electric fields, and of optoelectronic devices, such as electro-luminescence devices, avalanche photodiodes etc.

**Acknowledgments**

We are grateful to Brazilian Agencies CAPES, Fapesp, CNPq and Faep-Unicamp for partial financial support. One of the authors (LEO) would like to acknowledge the Facultad de Física de la Universidad de La Habana and the Ministério de Educación Superior de Cuba for local hospitality.

## References

[1] Goossen K W, Cunningham J E and Jan W Y 1990 *Appl. Phys. Lett.* **57** 2582
Feldmann J, Goossen K W, Miller D A B, Fox A M, Cunningham J E and Jan W Y 1991 *Appl. Phys. Lett.* **59** 66
Goossen K W, Cunningham J E, Williams M D, Storz F G and Jan W Y 1992 *Phys. Rev.* B **45** 13 773
Brener I, Knox W H, Goossen K W and Cunningham J E 1993 *Phys. Rev. Lett.* **70** 319
[2] Merlin R, Bajema K, Clarke R, Juang F Y and Bhattacharya P K 1985 *Phys. Rev. Lett.* **55** 1768
[3] Merlin R, Bajema K, Nagle J and Ploog K 1987 *J. Physique Coll.* **48** C5 503
[4] Laruelle F and Etienne B 1988 *Phys. Rev.* B **37** 4816
[5] Yamaguchi A A, Saiki T, Tada T, Nnomiya T, Misawa K, Kobayashi T, Kuwata-Gonokami M and Yao T 1990 *Solid State Commun.* **75** 955
[6] Munzar D, Bočáek L, Humlíček J and Ploog K 1994 *J. Phys.: Condens. Matter* **6** 4107
[7] Wang Y Y and Maan J C 1989 *Phys. Rev.* B **40** 1955
[8] Toet D, Potemski M, Wang Y Y, Maan J C, Tapfer L and Ploog K 1991 *Phys. Rev. Lett.* **66** 2128
[9] Bruno-Alfonso A, Oliveira L E and de Dios-Leyva M 1995 *Appl. Phys. Lett.* **67** 536
de Dios-Leyva M, Bruno-Alfonso A and Oliveira L E 1997 *J. Phys.: Condens. Matter* **9** 1005
[10] Kazarinov R F and Suris R A 1972 *Sov. Phys.–Semicond.* **6** 121
[11] Bleuse J, Bastard G and Voisin P 1988 *Phys. Rev. Lett.* **60** 220
[12] Dignam M M and Sipe J E 1990 *Phys. Rev. Lett.* **64** 1797
[13] Yu R H 1994 *Phys. Rev.* B **49** 4673
[14] Bastard G, Ferreira R, Chelles S and Voisin P 1994 *Phys. Rev.* B **50** 4445
[15] Sun N G, Yuan D and Deering W D 1995 *Phys. Rev.* B **51** 4641
[16] Mendez E E, Agullo-Rueda F and Hong J M 1988 *Phys. Rev. Lett.* **60** 2426
[17] Voisin P, Bleuse J, Bouche C, Gaillard S, Alibert C and Regnery A 1988 *Phys. Rev. Lett.* **61** 1639
[18] Agullo-Rueda F, Mendez E E, Ohno H and Hong J M 1990 *Phys. Rev.* B **42** 1470
[19] Bradshaw J L and Leavitt R P 1994 *Phys. Rev.* B **50** 17 666
[20] Agullo-Rueda F, Mendez E E and Hong J M 1989 *Phys. Rev.* B **40** 1357
[21] Laruelle F, Paquet D, Joncour M C, Jusserand B, Barrau J, Mollot F and Etienne B 1990 *Localization and Confinement of Electrons in Semiconductors (Springer Series in Solid State Science 97)* ed F Kuchar, H Heinrich and G Bauer (Berlin: Springer) p 258
[22] Laruelle F, Etienne B, Barrau J, Khirouni K, Brabant J C, Amand T and Brouseau M 1990 *Surf. Sci.* **228** 92
[23] de Brito P E, da Silva C A A and Nazareno H N 1995 *Phys. Rev.* B **51** 6096
[24] Castro M and Domínguez-Adame F 1997 *Phys. Lett.* **225A** 321
[25] MacDonald A H 1987 *Interfaces, Quantum Wells, and Superlattices* ed C R Leavens and R Taylor (New York: Plenum) p 347
[26] Brennan K F and Summers C J 1987 *J. Appl. Phys.* **61** 614
[27] de Dios-Leyva M, López-Gondar J and Bruno A 1992 *Phys. Status Solidi* b **169** 351
[28] Price P J 1986 *Superlatt. Microstruct.* **2** 593
[29] Landau L D and Lifshitz E M 1981 *Quantum Mechanics, Nonrelativistic Theory* (New York: Pergamon) p 555